University Library

MINERVA ACCESS

A gateway to Melbourne's research publications

Minerva Access is the Institutional Repository of The University of Melbourne

Author/s:
Micati, DJ;Radhakrishnan, K;Young, JC;Rajpert-De Meyts, E;Hime, GR;Abud, HE;Loveland, KL

Title:
'Snail factors in testicular germ cell tumours and their regulation by the BMP4 signalling pathway'

Date:
2020-09-01

Citation:
Micati, D. J., Radhakrishnan, K., Young, J. C., Rajpert-De Meyts, E., Hime, G. R., Abud, H. E. & Loveland, K. L. (2020). 'Snail factors in testicular germ cell tumours and their regulation by the BMP4 signalling pathway'. Andrology, 8 (5), pp.1456-1470. https://doi.org/10.1111/andr.12823.

Persistent Link:
https://hdl.handle.net/11343/275899

"Snail factors in testicular germ cell tumours and their regulation by the BMP4 signalling pathway"

Diana J. Micati [1,2], Karthika Radhakrishnan [1,2], Julia C. Young [1,2,6], Ewa Rajpert-De Meyts [3], Gary R. Hime [4], *Helen E. Abud [5,6], and *Kate L. Loveland [1,2, 6]

*Helen E Abud and Kate L Loveland are equal senior co-authors

1. Centre for Reproductive Health, Hudson Institute of Medical Research, Clayton, Victoria, Australia
2. Department of Molecular and Translational Sciences, Monash University, Clayton, Victoria, Australia
3. Department of Growth and Reproduction, Rigshospitalet, University of Copenhagen, Denmark
4. Department of Anatomy and Neuroscience, University of Melbourne, Melbourne, Australia
5. Stem cells and Development Program, Monash Biomedicine Discovery Institute, Monash University, Clayton, Victoria, Australia
6. Department of Anatomy and Developmental Biology, Monash Biomedicine Discovery Institute, Monash University, Clayton, Victoria, Australia

Correspondence should be addressed to K.L.

Phone +61 3 8572-2904

Address: Level 4 MHRP, 27-31 Wright Street, Hudson Institute of Medical Research, Clayton, 3168 Australia

Email: kate.loveland@monash.edu

Running title: Snail transcription factors in human germ cells

Funding information: This work was supported by grants from the National Health and Medical Research Council of Australia (Project grant ID1048110 to GH, HA, KL and Fellowship ID1079646 to KL)

Keywords: Snail transcription factors, human spermatogenesis, testicular germ cell tumours, TGF-β superfamily, importin 5

Abstract

This is the author manuscript accepted for publication and has undergone full peer review but has not been through the copyediting, typesetting, pagination and proofreading process, which may lead to differences between this version and the Version of Record. Please cite this article as doi: 10.1111/andr.12823

This article is protected by copyright. All rights reserved

Author Manuscript

Background: Snail transcription factors mediate key cellular transitions in many developmental processes, including spermatogenesis, and their production can be regulated by TGF-β superfamily signalling. SNAI1 and SNAI2 support many cancers of epithelial origin. Their functional relevance and potential regulation by TGF-β superfamily ligands in germ cell neoplasia are unknown.

Methods: SNAI1, SNAI2 and importin 5 (IPO5; nuclear transporter that selectively mediates BMP signalling) cellular localisation was examined in fixed normal adult human and/or neoplastic testes using *in situ* hybridisation and/or immunohistochemistry. SNAI1 and SNAI2 functions were assessed using the well characterised human seminoma cell line, TCam-2. Cell migration, adhesion/proliferation, and survival were measured by scratch assay, xCELLigence and flow cytometry following siRNA-induced reduction of *SNAI1* and *SNAI2* in TCam-2 cells. The potential regulation of *SNAI1* and *SNAI2* in TCam-2 cells by TGF-β signalling ligands, activin A and BMP4, was evaluated following 48 hours culture, including with siRNA regulation of IPO5 to selectively restrict BMP4 signalling.

Results: In normal testes, *SNAI1* transcript was identified in some spermatogonia and in spermatocytes, and SNAI2 protein localised to nuclei of spermatogonia, spermatocytes and round spermatids. In neoplastic testes, both *SNAI1* and SNAI2 were detected in GCNIS and in seminoma cells. SNAI1 and SNAI2 reduction in TCam-2 cells by siRNAs significantly inhibited migration and survival, respectively. Exposure to BMP4, but not activin A, significantly increased *SNAI2* (~18-fold). *IPO5* inhibition by siRNAs decreased BMP4-induced *SNAI2* upregulation (~5-fold). Additionally, *SNAI2* reduction using siRNAs inhibited BMP4-induced TCam-2 cell survival.

Conclusions: This is the first evidence that SNAI1 and SNAI2 are involved in human spermatogenesis, with independent functions. These outcomes demonstrate that SNAI1 and SNAI2 inhibition leads to loss of migratory and viability capacities in seminoma cells. These findings show the potential for therapeutic treatments targeting SNAIL or BMP4 signalling for patients with metastatic testicular germ cell tumours.

Introduction

This article is protected by copyright. All rights reserved

Author Manuscript

Snail proteins belong to a family of zinc-finger transcription factors that play crucial roles in cell migration, chromatin remodelling and cell signalling to impact on many biological processes in normal embryonic development and tumorigenesis (1, 2). The three Snail factors exert their functions through tight transcriptional regulation. Their highly conserved C-terminal region contains 4 to 6 zinc fingers in a DNA-binding domain which interacts directly with target genes. Once bound, Snail proteins recruit several co-factors through their N-terminal SNAG domain; these are mainly chromatin remodelling enzymes that directly repress or activate gene activity depending on cell-context (1, 3, 4).

There is limited information from studies of the adult mouse testis to suggest Snail factors mediate key cellular transitions by controlling changes in gene expression. In adult mice, aberrant *Snai1* or *Snai2* synthesis disrupted spermatogenesis. Specifically, analysis of ubiquitin ligase *β-Trcp* knockout mice provided indirect evidence that elevated SNAI1 in spermatogonia can cause germ cell loss (5). A testicular phenotype was reported in mice lacking *Snai2* at six weeks of age, with testicular atrophy resulting from an apparent reduction in germ cell number (6). However, no further characterisation of these testes is available. We previously identified the precise cellular sites of Snail transcription factor activity in the postnatal mouse testis, revealing distinct and dynamic profiles for each. SNAI1 and SNAI2, not SNAI3, were detected in the nucleus of germ cells at different stages of maturation. They co-localised with chromatin remodelling enzymes, such as LSD1 and PRC2 components (7), and thus mediate transcriptome reprogramming during spermatogenesis (8, 9).

Snail functions are well defined in epithelial cells. By regulating epithelial cell gene expression, Snail factors can induce an epithelial to mesenchymal transition (EMT) (10) in which an epithelial cell acquires the migratory and invasive capacities of a mesenchymal cell (11). EMT is required for normal embryonic development, but in adults, Snail-induced reduction of epithelial markers, such as *CDH1*, is a hallmark of tumour initiation, providing cancer cells with the ability to migrate from the primary tumour and metastasise to distant sites (12).

Snail activities also contribute to normal tissue homeostasis and cancer progression, as elevated Snail levels drive cells to acquire stem cell properties. In mouse small intestinal epithelium, Snai1 expression is localised to the stem cell population where it is required for their maintenance (13, 14). Increased Snail levels promote a stem cell-like phenotype in various cancers including those of the breast epithelium (15) and human pancreas (16); this allows cancer cells to adopt self-renewing capacities, become chemotherapy resistant and metastatic

This article is protected by copyright. All rights reserved

Author Manuscript

and cause relapse (17). Snail overexpression can also increase proliferation of human glioblastoma cells (18) and support survival of two gastrointestinal stromal tumour cell lines by regulating pro-apoptotic and anti-apoptotic gene activity (19). As Snail proteins function beyond EMT, it is evident that they promote cancers of non-epithelial origins, such as testicular germ cell tumours (TGCTs).

TGCTs arise from a common precursor cell known as germ cell neoplasia *in situ* (GCNIS), first described as an atypical spermatogonia in testicular biopsies of patients who subsequently developed testicular cancer (20). Similarities in morphology and gene expression profiles between GCNIS and human foetal germ cells indicates that GCNIS originates from an early gonocyte that has failed to differentiate, but persists in adulthood (21, 22). Unknown events that occur at puberty drive GCNIS cells to proliferate and progress into one of the two malignant TGCTs (23): either seminoma or non-seminomas, the latter characterised by loss of germ cell phenotype and activation of somatic differentiation. Among men with TGCTs, approximately 50% are diagnosed with seminomas (24, 25) which histologically appear as undifferentiated cells that resemble GCNIS with characteristic lymphocytic infiltration in the supporting stroma.

The Transforming Growth Factor (TGF-β) signalling pathway is central to testis development and reproductive health (26), in addition to embryogenesis and tumorigenesis (27, 28). Briefly, activin A binding to serine/threonine kinase receptor subunits induces phosphorylation of SMADs 2 and/or 3. In contrast, BMP4 binding to cognate receptors, including those shared with activin, leads to phosphorylation of SMAD 1/5/9 (29). Once phosphorylated, SMADs bind to SMAD4 forming a trimeric complex which is transported into the nucleus to activate target gene transcription in concert with specific co-factors (30, 31). Protein transport from the cytoplasm into the nucleus is mediated by importins (32). IPO5 is one of the several importin molecules readily detected in the embryonic and postnatal mouse testis (33, 34), and in the normal adult human testis (35). Its dynamic and cell-specific expression profile suggests that IPO5 plays a role during major developmental switches, potentially influencing testis development and sperm production. Recent studies identified IPO5 as an intracellular mediator of the BMP4 signalling pathway translocates SMADs 1/5/9, but not SMADs 2/3, from cytoplasm to nucleus initiating transcription of BMP4 target genes (36). Thus, the selective transport of SMADs 1/5/9 by IPO5 indicates its expression and function is particularly important as a BMP4 signalling mediator; its presence and role in TGCTs is yet to be elucidated.

This article is protected by copyright. All rights reserved

Author Manuscript

Several lines of evidence link aberrant TGF-β signalling with TGCT progression. Elevation of the activin A type II receptor in the adult testis is observed only within seminoma cells (37), and upregulation of activin inhibitors, betaglycan and inhibin (38), is also detected in some seminoma samples. This highlights the potential involvement of disrupted activin signalling in TGCT. Altered BMP signalling in TGCT is indicated by BMPR expression in paediatric seminomas/germinomas (39) and mutation in activin receptor-like kinase (*alk6b*), a BMP receptor, in zebrafish germ cell tumours (40). An important model of human seminoma with early gonocyte features, the TCam-2 human seminoma cell line, responds differentially to activin A and BMP4 (41). It features hallmarks of early foetal germ cells and primary seminoma tumours including PRDM1 (BLIMP1), KIT, OCT3/4, SOX17, AP2γ, and NANOG (42). Activin A treatment of TCam-2 cells significantly increases *KIT* transcript level, while exposure to BMP4 increases survival (41), indicating the TGF-β superfamily pathway regulates transcription of factors associated with germ cell development. Snail transcription factor levels are regulated by the TGF-β superfamily (11) in the uterus to allow extravillus cytotrophoblasts invasion of the endometrium to support placental development (43). In the oesophagus, BMP4-induction of *SNAI2* expression mediate the transformation of premalignant squamous epithelial cells into oesophageal adenocarcinoma (44). However, Snail regulation mediated by activin A or BMP4 in seminomas has not been studied.

The present study was performed to investigate how Snail transcription factors may influence TGCT initiation and progression. For the first time, we provide evidence that SNAI1 and SNAI2 are present in germ cells of the normal adult human testis, supporting the hypothesis that Snail transcription factors might regulate gene expression changes at key spermatogenic stages, as previously documented in mice. Identification of SNAI1 and SNAI2 in GCNIS and seminomas suggests that Snail factors contribute to TGCT initiation and progression. To address their functions in cell migration, proliferation, adhesion and survival, TCam-2 cells were used and treatment of TCam-2 cells with activin A and BMP4 identified a potential mechanism for Snail regulation.

Materials and Methods

Histological analysis of normal and neoplastic human testis samples

Snail transcript and protein expression patterns were analysed using 4 μm thick, Bouin's or PFA fixed, paraffin-embedded sections of normal adult human testis, GCNIS with or without

This article is protected by copyright. All rights reserved

Author Manuscript

areas of normal spermatogenesis, and seminomas. GCNIS and seminoma tissue samples employed in this study were derived from adult male patients, ranging between 27 and 55 years old. All procedures involving normal adult human testis and TGCT samples were approved by the Monash University Human Research Ethics Committee and the Regional Committee for Medical Research Ethics (Copenhagen), respectively.

DIG-labelled RNA probes and *in situ* hybridisation

DIG-labelled RNA probes for *in situ* hybridisation were originally generated from RT-PCR products (primer sequences in Table 1) cloned into the pGEM-T-Easy vector (Promega, Madison, WI, USA) and validated by sequencing (Gandel Genomics Centre, Monash Health Translation Precinct). These plasmids were amplified by RT-PCR using pBS forward and reverse primers to create templates for *in vitro* transcription to generate sense and antisense cRNA probes.

In situ hybridisation was used to detect *SNAI1* and *SNAI2* in Bouin's fixed section of human testis samples used standard procedures (7). In brief, hybridisation was performed with 3 µg/ml probe diluted in *in situ* hybridisation buffer at 55°C overnight. Bound-cRNA probe was detected using an alkaline phosphatase-labelled-anti-DIG antibody (1:1000 in 10 X DIG blocking buffer, Roche) and visualised using a substrate for alkaline phosphatase (BCIP/NBT, Thermo Fisher Scientific). Sections were counterstained with Harris haematoxylin (Sigma-Aldrich) and mounted with GVA aqueous mounting solution (Genemed, San Francisco, CA, USA). *In situ* hybridisation was performed using the *SNAI1* cRNA probes on 2 and 3 normal adult and neoplastic human samples, respectively. The *SNAI2* antisense cRNA probe was used to detect *SNAI2* transcript in normal adult human testes only. SNAI2 expression pattern in normal and neoplastic adult human samples was further delineated by immunohistochemistry using an anti-SNAI2 antibody as described below.

Immunohistochemistry

Immunostaining was performed to localise SNAI2 in the normal adult human testis and TGCTs, and IPO5 in TGCTs. The SNAI2 antibody used in this study was previously validated on *Snai2* knockout mouse testis samples (7); the IPO5 antibody was previously used on adult human testis and validated by Western blot using HeLa cells and adult mouse testis lysates (35). SNAI2 and IPO5 antibodies were applied using a standard protocol.

Briefly, Bouin's fixed sections were dewaxed and rehydrated, then placed in antigen retrieval solution (SNAI2 probed sections in 10 mM Citrate Buffer, pH 6.0; IPO5 probed sections in 50

This article is protected by copyright. All rights reserved

Author Manuscript

mM Glycine, pH 3.5) for 10 minutes in a 1000W Pressure Cooker (Tefal). After cooling to room temperature (RT), the sections were treated with 0.3% hydrogen peroxide for 5 minutes at RT, then washed twice for 5 minutes at RT in Tris-buffered saline (TBS; 50 mM Tris, 150 mM NaCl, pH 7.5). Blocking solution consisted of CAS Block (Invitrogen, Thermo Fisher Scientific) for 1 hr at RT in a humid chamber. Sections were incubated with anti-SNAI2 (Abcam, ab27568, 1:200, diluted in CAS Block) or anti-IPO5 (Santa Cruz, sc-11369, 1:1500, diluted in CAS Block) overnight at RT and at 4°C, respectively, then with biotinylated anti-rabbit secondary antibody (Invitrogen, #656140, 1:500, in CAS Block). Signal was amplified using Vectastain Elite ABC kit reagents following the manufacturer's instructions (Vector Laboratories, Burlingame, CA, USA), then a brown reaction product detected with DAB (3,3-diaminobenzidine tetrahydrochloride, DAKO, Steinheim, USA). Sections were counterstained using Harris haematoxylin, dehydrated and mounted using Dibutylphthalate Polystyrene Xylene (DPX) (Sigma-Aldrich). Control sections lacked primary antibody to observe non-specific secondary antibody binding. SNAI2 immunostaining antibody was performed on 2 normal adult human testes, 3 GCNIS and 3 seminoma samples, and IPO5 in 3 GCNIS and 4 seminoma samples.

TCam-2 cell line culture

The TCam-2 cell line, derived from a human seminoma (45), has been characterised as an appropriate model for studies of human seminoma (46), primordial germ cells, and early gonocytes (41). TCam-2 cells were maintained at 37°C (5% CO_2) in growth medium consisting of RPMI 1640 medium (Gibco) containing 10% foetal calf serum (FCS; Bovogen, New Zealand) with 0.5% Penicillin/Streptomycin (Pen/Strep, Gibco) and passaged at 90% confluency.

Immunofluorescence on fixed TCam-2 cells

Immunofluorescence detection of SNAI1 and SNAI2 in TCam-2 cells was performed on cells seeded in a 12 well tissue culture plate on 12 mm round glass coverslips (Menzel) at 1 x 10^5 cells/well and cultured overnight. Once confluent, cells were rinsed in phosphate buffered saline (PBS; Gibco), then fixed in 4% PFA for 10 minutes. Coverslips were rinsed in PBS, cells permeabilised in 0.1% Triton-X 100/PBS (Merck, Darmstadt, Germany) for 10 minutes and 0.5% Bovine Serum Albumin (BSA, Sigma-Aldrich)/PBS was added for 1 hour at RT to block non-specific binding. Cells were incubated with primary antibodies diluted in 0.5% BSA/PBS overnight at RT. Primary antibodies used were: anti-SNAI1 (Cell Signalling,

This article is protected by copyright. All rights reserved

Author Manuscript

C15D3, 1:100) and anti-SNAI2 (Abcam, ab27568, 1:100). The following day, cells were washed 3 times in PBS, then Alexa Fluor 546 goat anti-rabbit (Invitrogen, A11010, 1:500 in 0.5% BSA/PBS) secondary antibody was applied for 1 hr at RT. Cells were rinsed in PBS and stained with 300 nM DAPI (Molecular Probes, Invitrogen) diluted in PBS for 5 minutes, rinsed in PBS and mounted on slides under GVA. The specificity of the SNAI1 antibody is evident from over 183 publications, including by western blot (47). The SNAI2 antibody was validated as discussed above.

Transfections

TCam-2 cells were seeded in 6 well plates (2 X 10^5 cells/well), then incubated overnight in growth medium to reach 60% confluency. Medium was replaced with RPMI + 5% FCS, lacking Pen/Strep. Transfections used the Lipofectamine™ RNAiMAX system (Invitrogen) following manufacturer's instructions. Pre-designed small interfering RNAs (siRNAs) (Silencer select siRNA, Thermo Fisher) were used to selectively reduce *SNAI1* (Invitrogen, 5 nmol, Cat #4392420, ID #s13187), *SNAI2* (Invitrogen, 5 nmol, Cat #4392420, ID # s13128), and *IPO5* (Invitrogen, 5 nmol, Cat #4392420, ID S7935). Following dose-response testing, the *SNAI1* siRNA construct was used at a final concentration of 25 pmol/well of 6 well plate and *SNAI2* and *IPO5* siRNA constructs were used at 12.5 pmol/well. The Silencer Select Negative Control siRNA *SCRAMBLE* (*SCRAM*) (Thermo Fisher, 40 nmol, Cat # 4390844) served as controls in each experiment. To validate transfection efficiency, TCam-2 cells were collected 1 and 4 days post-transfections in TRIzol (Ambion, Life Technologies, Carlsbad, CA, USA). Efficiency of gene knockdown was assessed by qRT-PCR. All experiments were independently reproduced at least 3 times.

Migration assay

TCam-2 cells were grown to confluence in 6 well plates, then a cell free gap was generated across the well using a P200 pipette tip. Growth medium was replaced with RPMI + 5% FCS lacking Pen/Strep. Transfections were performed immediately after wound formation. Three indicator marks per well were drawn on the plate bottom to determine specific regions of the gap for subsequent imaging. Plates were photographed using a 4X objective at 0 hrs, then again at 1, 2, 3, and 4 days post-gap formation to assess migration. The percentage of gap size normalised to 0 hrs was determined by measuring the wound area using Image J. All experiments were performed on 3 separate occasions.

Viability Assay

This article is protected by copyright. All rights reserved

Author Manuscript

Two and three days post-transfections, TCam-2 cells were harvested using 0.1% trypsin/versene (TV; 2.5% trypsin, diluted in PBS/EDTA, Gibco), rinsed in PBS and resuspended in 5% FCS/PBS containing 0.05 mg/ml propidium iodide (PI, 5 mg/ml, Sigma-Aldrich). The viable to non-viable cell ratio based on PI incorporation was measured on the LRS-Fortessa X-20 Analyser (gated at B710-A) at the Monash University Bioplatform Flowcore Facility – MHTP node. Three independent experiments were performed. The results are graphed as fold-change in non-viable cells, relative to the *SCRAM* siRNA control value. All experiments were repeated on 3 separate occasions.

Real-time monitoring of TCam-2 cell adhesion/proliferation

TCam-2 cells were seeded in 6 well plates and transfected at confluency in RPMI + 5% FCS lacking Pen/Strep. One-day post-transfections, TCam-2 cells were detached using TrypLE Express (Gibco) at 37°C for 5 minutes, and the reaction was quenched by adding medium. A 150 µl suspension of 1 x 10^4 cells was added to each well of an E-plate (16 wells) (ACEA Biosciences, San Diego, CA). For this assay, cells were maintained in RPMI + 5% FCS. The E-plate was loaded onto the xCELLigence System Real-Time Cell Analyser (RTCA; Roche) in a 37°C incubator, and adhesion/proliferation measured by monitoring the impedance value (Cell Index, CI) of each well every 15 minutes over 3 days. In simplest terms, the greater the CI value, the greater the level of cell adhesion. Conversely, when the CI decreases, the net adhesion is decreased. The cell growth rate was calculated from the slope of the line between values at specific time points. Four independent experiments were performed.

EdU (5-ethynyl-2'-deoxyuridine) incorporation to measure proliferation

Three days post-transfection, medium was replaced with RPMI + 5% FCS containing 10 µM EdU (Click-iT, EdU Flow Cytometry Assay Kit, Invitrogen). Cells were incubated at 37°C for 2 hrs, detached using TrypLE Express for 5 minutes and the reaction quenched. Cells were pelleted, resuspended in 4% PFA/PBS, and fixed at RT for 10 minutes. After rinsing three times in PBS, EdU staining was performed following the manufacturer's protocol. The ratio of proliferative to non-proliferative cells, based on EdU incorporation, was measured by flow cytometry (LRS-Fortessa X-20 Analyser at the Monash University Bioplatform Flowcore Facility – MHTP node). Data are presented as mean values, collected in duplicate experiments. Results are shown as fold-change relative to values obtained for the *SCRAM* siRNA control sample.

Activin A and BMP4 treatments of TCam-2 cells

This article is protected by copyright. All rights reserved

Author Manuscript

To determine the signalling pathways that regulate *SNAI1* and *SNAI2* transcripts, TCam-2 cells were seeded in a 12 well plate and incubated in growth medium. Once confluent, cells were serum starved (grown in RPMI alone) for 12 hrs, then treated with activin A (AA) (R&D Systems Inc, Minneapolis, USA) and BMP4 (R&D Systems Inc, Minneapolis, USA), diluted in RPMI only medium. A dose-response test (Fig. S3) was performed to determine the final concentration of AA and BMP4 to use. TCam-2 cells were serum-starved overnight, then treated with 2.5, 5, 10 and 20 ng/ml of AA or BMP4. Forty-eight hours post-treatment, TCam-2 cells were collected to measure *SNAI1* and *SNAI2* transcript levels by qRT-PCR. *SNAI1* (Fig. S3 A, B) and *SNAI2* (Fig. S3 C, D) transcript levels reached a plateau at 5 ng/ml, suggesting this as the optimal concentration of AA or BMP4 to use in this study. An equivalent volume of diluent (4 mM HCl/BSA) was used as vehicle control. Forty-eight hours post-treatment, TCam-2 cells were collected in TRIzol (Ambion) and Snail transcript levels were measured by qRT-PCR. All experiments were repeated on 3 separate occasions. To delineate whether IPO5 is required to mediate AA or BMP4 cellular responses, TCam-2 cells were seeded in a 12 well plates, incubated in RPMI + 10% FCS + 0.5% Pen/Strep until 60% confluent, then transfected with *SCRAM* or *IPO5* siRNAs. Twenty-four hours post-transfections, TCam-2 cells were serum-starved for 12 hours, then treated with 5 ng/ml of AA or 5 ng/ml of BMP4 for 48 hours. The *SCRAM* siRNA and vehicle were used as transfection and treatment controls, respectively. TCam-2 cells were then collected in TRIzol (Ambion) and *SNAI1* and *SNAI2* transcripts were measured by qRT-PCR. All experiments were repeated 3 times.

Migration assay following *IPO5* or *SNAI2* knockdown, and AA or BMP4 treatments

TCam-2 cells were seeded in 6 well plates, incubated overnight until confluent and transfected with 12.5 pmol of *SCRAM* and *SNAI2* or *IPO5* siRNA constructs. Twenty-four hours post-transfections, cells were serum-starved (grown in RPMI alone) for 12 hrs, then SNAI2 transfected cells were treated with 5 ng/ml of AA or BMP4, where IPO5 transfected TCam-2 cells were treated with 5 ng/ml of BMP4 only. A single scratch was generated across the well and the closure of the gap size was measured over 3 days. The *SCRAM* siRNA construct and vehicle were used as transfection and treatment controls, respectively. Percentage of gap size normalised to 0 hrs was determined by measuring the wound area using Image J. All experiments were performed on 3 separate occasions.

Quantitative Real-Time PCR (qRT-PCR)

This article is protected by copyright. All rights reserved

Author Manuscript

Following RNA extraction using TRIzol, TCam-2 RNA samples were treated with the DNase-free kit (Invitrogen Life Technologies, Oregon, USA) following the manufacturer's specifications. First strand cDNA synthesis was performed with 50 μM random hexamers (Promega, Madison, WI, USA) and 10 μM dNTPs (Sigma, St Louis, MO) for 500 ng of RNA/sample. Samples were incubated at 65°C for 5 minutes to denature RNA, placed on ice, then 0.1 M DTT, First Strand Buffer and Superscript III Reverse Transcriptase (Invitrogen, 200 U/μl) were added for incubation at 50°C for 1 hr. Enzymes were inactivated at 70°C for 15 minutes. Negative control reactions lacking Superscript III were included for each sample. Quantitative Real-Time PCR was performed on the Applied Biosystems 7900HT Sequencing Detection machine (Applied Biosystems, Medical Genomics Facility, Monash Health Translation Precinct) at 95°C for 10 minutes, with 45 cycles of amplification at 95°C for 15 seconds, and 62°C for 30 seconds. Reactions were standardised against TCam-2 cDNA diluted 1:10, 1:40, 1:160, 1:640, 1:2560 in filtered MilliQ water. Following qRT-PCR, results were analysed using the SDS Automatic Controller 2.3 (Applied Biosystems). Three independent experiments were performed for each primer pair, with error bars indicating standard error of the means (SEM). The sequences are listed in Table 1.

Statistical analyses

Values from control versus treated samples are presented as 3 or 4 independent experimental results, as described in each figure legend. Mann-Whitney test, and non-parametric ANOVA and Tukey's multiple comparison test were performed using GraphPad Prism™, with $p < 0.05$ determining significance.

Results

SNAI1 and SNAI2 have distinct expression profiles within the normal adult and neoplastic human testis

Our previous investigation of the postnatal mouse testis revealed that each Snail family member has a distinct cellular expression profile in somatic and germline cells (7), with SNAI1 and SNAI2 developmentally regulated in spermatogenic cells. We examined whether Snail expression is conserved in adult human testis. In the absence of an antibody suitable for SNAI1 detection in paraffin embedded human tissue samples, we employed *in situ* hybridisation using a validated probe and observed *SNAI1* transcript in some, but not all spermatogonia,

This article is protected by copyright. All rights reserved

Author Manuscript

spermatocytes and peritubular cells, with a faint signal detected in Sertoli cells. Round and elongated spermatids contained no detectable *SNAI1* transcript (Fig. 1A, Fig. S1). *In situ* hybridisation for detection of *SNAI2* transcript identified a signal in spermatogonia, spermatocytes, round spermatids and Sertoli cells of the normal adult human testes (Fig. 1B). Further immunohistochemical analysis of normal adult human testis revealed SNAI2 expression to be stage-specific with nuclear signal evident in some A_{dark} and A_{pale} spermatogonia, late pachytene spermatocytes and round spermatids; elongated spermatids were negative. Additionally, some Sertoli cell nuclei, peritubular and interstitial cells exhibited SNAI2 immunostaining (Fig. 1C, Fig. S2). These data suggest that SNAI1 and SNAI2 are active during major cellular transitions that occur during spermatogenesis and identify germ, Sertoli and peritubular cells as common sites for Snail production within the normal adult human testis.

As Snail transcription factors are central to the induction of many cancers (48-50), we further investigated their expression in testicular samples containing neoplasms that retain the phenotypic features of germ cells; GCNIS and seminomas. *In situ* hybridisation demonstrated *SNAI1* mRNA in some premalignant GCNIS cells (Fig. 1D, Fig S1). In seminomas, *SNAI1* was identified in seminoma cells and in the somatic cells around them (Fig. 1F, S1). Immunohistochemical analysis of GCNIS samples showed strong SNAI2 in some GCNIS cell nuclei, peritubular cells and in the extracellular matrix component (ECM) with no signal evident in interstitial cells (Fig. 1E, S2 B). SNAI2 was detected as an intense signal in the nuclei of seminoma cells in every sample (Fig. 1G, Fig. S2). Interestingly, only two of the samples analysed showed nuclear SNAI2 within cells which resemble immune infiltrates (Fig. 1G, Fig. S2 D). Overall, these results indicate that SNAI1 and SNAI2 are both expressed in TGCTs.

The TCam-2 seminoma cell line as an *in vitro* model to assess the function of Snail proteins

To delineate the role of SNAI1 and SNAI2 in TGCTs, we evaluated the suitability of using the human TCam-2 seminoma cell-derived line as a model for *in vitro* analyses. We first interrogated their expression in TCam-2 cells. Existing RNASeq data (51) indicates that transcripts encoding SNAI1 and SNAI2, but not SNAI3, are present in TCam-2 cells (Fig. S4 A). This was further validated by immunofluorescence detection of nuclear SNAI1 and SNAI2 protein (Fig. 2A), which is in accord with their expression in seminoma cells (Fig. 1).

***SNAI1* loss increases *SNAI2* transcript levels**

This article is protected by copyright. All rights reserved

Author Manuscript

To establish conditions for identifying SNAI1 and SNAI2 functions in seminoma cells, we manipulated their levels in TCam-2 cells. *SNAI1* and *SNAI2* were reduced using siRNA constructs; knockdown efficiency was validated by qRT-PCR. *SNAI1* was significantly reduced following both 1 day (~ 55%) and 4 days (~ 50%) exposure to *SNAI1* siRNA, compared to *SCRAM* control sample levels (Fig 2B). *SNAI2* was significantly reduced to 70% 1 day post-transfection with *SNAI2* siRNA, however there was no significant difference from *SCRAM* control sample levels at 4 days (Fig 2C); this was considered as an indication that TCam-2 cells lacking *SNAI2* might not be viable and was tested below. We examined the potential for SNAI1 and SNAI2 to compensate for each other's loss in TCam-2 cells, as described during mouse chondrogenesis (52). In TCam-2 cells, lowering *SNAI1* levels significantly increased *SNAI2* at 4 days post-transfection (Fig 2B), however decreased *SNAI2* did not alter *SNAI1* (Fig 2 C). This identifies a potential feedback that can occur in seminoma cells between *SNAI1* and *SNAI2* transcripts.

SNAI1 mediates cell migration and SNAI2 supports survival of TCam-2 cells

To test specific potential functions of SNAI1 and SNAI2 in seminoma cells, TCam-2 behaviour was assessed following siRNA-mediated transfections. We initially employed a monolayer scratch assay to examine SNAI1 and SNAI2 in TCam-2 cell migration. Cells were grown in 5% FCS containing medium, a condition appropriate to support transfected cell growth throughout the 4 day culture period, without well overgrowth. A gap was created at day 0 of transfection and was measured daily. The gap size in the *SCRAM* controls reduced up to 50% within 4 days. In samples with reduced *SNAI1* levels, a significant decrease in gap closure (to ~ 80% of original size) was measured (Fig. 3A), while *SNAI2* knockdown resulted in a significant gap size increase between 2 and 4 days (up to ~ 125% by day 4) following transfection (Fig. 3A).

As a gap size larger than 100% suggests cell death has occurred in the sample, TCam-2 cell survival was measured by flow cytometry at 48 and 72 hrs post-transfection by propidium iodide incorporation. TCam-2 cell viability was significantly decreased by *SNAI2* reduction, compared to *SCRAM* control (Fig. 3B). Major contributing factors to cell death can include loss of cell adhesion and cell proliferation arrest. To assess this, TCam-2 cells were transfected with *SNAI1* and *SNAI2* siRNA constructs for 24 hrs, then adhesion analysed by xCELLigence every 15 minutes over 6 hours. Reduced *SNAI2* significantly decreased the proportion of adherent TCam-2 cells (Fig. 3C). An initial examination by xCELLigence (Fig. 3E) suggested

This article is protected by copyright. All rights reserved

Author Manuscript

that *SNAI2* knockdown significantly reduced the proportion of proliferating cells, however further assessment by EdU incorporation identified no changes in cell proliferation when measured at 72 hrs post-transfection (Fig. 3D). *SNAI1* reduction did not affect TCam-2 cell viability, adhesion or proliferation (Fig. 3 B – E).

SNAI2 transcript is elevated following stimulation with BMP4 but not activin A

We investigated candidate members of the TGF-β superfamily previously linked with early germline development an TGCT progression for their ability to drive expression of SNAI1 and SNAI2. TCam-2 cells were treated with either activin A or BMP4 (5 ng/ml), then *SNAI1* and *SNAI2* transcripts quantified. *SNAI1* levels were not significantly different in response to activin A or BMP4 (Fig. 4A). *SNAI2* was robustly increased by BMP4 treatment, but unaffected by activin A (Fig. 4B). This result identifies *SNAI2* as a selective target of BMP4 in seminoma cells.

IPO5, an intracellular BMP4 signalling mediator, regulates *SNAI2* expression

IPO5 was recently identified to selectively transport SMADs 1/5/9 into the nucleus of human liver cells to initiate BMP4-induced cellular responses (36). Immunohistochemistry identified IPO5 as predominantly cytoplasmic in GCNIS and Sertoli cells (Fig. S4A-C), while heterogenous cytoplasmic and nuclear distribution of IPO5 was apparent between the different seminoma samples analysed (Fig. 4C, D; Fig. S4D, E).

Published RNASeq data (51) showed that *IPO5* transcript levels are high in TCam-2 cell samples (Fig. S4F) and was observed that the protein is readily detected by immunofluorescence (data not shown). To investigate whether *SNAI2* elevation following BMP4 is mediated by IPO5, an siRNA construct targeting *IPO5* was introduced and effectively reduced *IPO5* levels (to < 95%, compared to *SCRAM* control levels) after 24 hrs (Fig. S4G). At 24 hrs following *IPO5* knockdown, TCam-2 cells were serum-starved for 12 hrs, then treated with either 5 ng/ml of activin A or BMP4. Cells were collected 48 hrs later and *SNAI1* and *SNAI2* transcript levels were quantitated. *IPO5* knockdown did not affect *SNAI1* expression following exposure to either factor (Fig. 4E), reinforcing evidence (Fig. 4A) that these signalling pathways do not alter *SNAI1* transcription. However, *IPO5* knockdown significantly reduces the BMP4-mediated increase in *SNAI2* (Fig. 4F). This reveals for the first time that IPO5 levels determine the outcome of BMP4 signalling and specifically affect *SNAI2*.

BMP4-induced survival of TCam-2 cells is modulated by *SNAI2*

This article is protected by copyright. All rights reserved

Author Manuscript

441 BMP4 signalling pathway was shown to support TCam-2 seminoma cell survival (41). To
442 determine whether SNAI2 contributes to BMP4-induced cellular response, we transfected
443 TCam-2 cells with the *SNAI2* siRNA constructs. Cells were serum-starved for 12 hrs, then
444 treated with 5 ng/ml of vehicle control, activin A or BMP4 for 3 days. The functional response
445 was assessed with a migration assay as described above, where a gap size larger than 100% of
446 original size indicates cell death. Vehicle (control) treatment following *SNAI2* knockdown
447 resulted in a significant increase in gap size (~ 110% of original gap size) compared to the
448 *SCRAM* control (reduced to ~ 80%) (Fig. 4G), indicating that reduced *SNAI2* levels result in
449 TCam-2 cell death, as expected and previously shown (Fig. 3 A, B). Activin A treatment of
450 TCam-2 cells following *SNAI2* knockdown resulted in gap closure (Fig. 4H); this confirms that
451 *SNAI2* is not a downstream target of activin A and suggests that activin A can support TCam-
452 2 cell migration, even when *SNAI2* is reduced. Interestingly, BMP4 treatment following *SNAI2*
453 knockdown resulted in a significant increase in gap size (~ 110%) (Fig. 4I), demonstrating that
454 BMP4 is unable to rescue the effects of *SNAI2* knockdown. These results further indicate that
455 SNAI2 is required for BMP4-induced survival in TCam-2 cells and confirm *SNAI2* as a
456 downstream target of the BMP4 signalling pathway.

457 To determine whether IPO5 is implicated in the signal transduction pathway proposed above,
458 TCam-2 cells were transfected with *IPO5* siRNA. Cells were serum-starved for 12 hours, then
459 treated with 5 ng/ml of the vehicle (control) or BMP4. Functional response was assessed using
460 a scratch assay, where the gap size was measured over a period of 3 days. Vehicle (control)
461 and BMP4 treatments following *IPO5* knockdown, showed a significant decrease in gap
462 closure (to ~ 95% of original gap size) compared to *SCRAM* siRNA control (Fig. 4 J, K). These
463 results suggest that reduction in *IPO5* levels did not affect BMP4-induced cell survival as
464 drastically as observed following the *SNAI2* knockdown (Fig. 4 I). As demonstrated by qRT-
465 PCR, *IPO5* knockdown significantly reduced the BMP4-induced increase in *SNAI2*, however
466 *SNAI2* transcript levels remained higher than in the vehicle control (Fig. 4F). This indicates
467 that a lower level of *SNAI2* can partially support TCam-2 cell survival.

468

469 **Discussion**

470 Evidence implicating Snail transcription factors in mammalian spermatogenesis is limited. The
471 current study was performed to understand how Snail factors may influence normal and
472 neoplastic germ cells in the adult human testis. It is known from *Drosophila* studies that

This article is protected by copyright. All rights reserved

Author Manuscript

Escargot, one of the three Snail members, is expressed in the somatic hub cells, cyst stem cells (CySCs) and germline stem cells (GCS) of the adult testis; its knockdown indicated that it is required in hub cells to maintain niche integrity (53). A distinct profile for SNAI1 and SNAI2 in spermatogenic cells of the postnatal mouse testis and their co-localisation with chromatin remodelling enzymes, identified their potential involvement in germ cell transitions through each spermatogenic stage, where tight control of gene expression is essential (7). Aberrant *Snai1* and *Snai2* levels result in germ cell loss (5, 6), implicating regulations of Snail levels are important in spermatogenesis. This study demonstrates that expression profiles of SNAI1 and SNAI2 in spermatogenic cells are grossly conserved between mouse and human adult testes, however the heterogeneity observed in SNAI1 and 2 expression in the human testis presents an interesting contrast to the more homogeneous expression in the mouse testis. Multiple studies have identified considerable transcriptional heterogeneity across the spermatogonial stem cell population in mammals; some examples include (54-58). These high stringency single-cell level observations are increasing in frequency with more recent analyses of human samples. The data presented in the current study is consistent with the single cell RNAseq data in (59) study, in which human SSCs express SNAI1 and SNAI2 transcripts in around 5% of SSEA4 positive SSCs (data available as GSE92276). A similarly heterogeneous expression pattern in human SSCs was observed by Hermann et al 2018 (accessible at (60), "Queryable single-cell RNA-seq (10x Genomics) datasets of Human and Mouse spermatogenic cells", Mendeley Data, v1http://dx.doi.org/10.17632/kxd5f8vpt4.1). The direct functional implications of this heterogeneity are beyond the scope of the present study, but may indicate there are differential roles for individual SNAIs in the 3-10 clusters of SSC subpopulations, as defined by some of the studies above (reviewed in (61)). The tight regulation of SNAI transcription factors in spermatogenesis is an ongoing area of interest for our lab.

Despite the widespread use of mice for studies examining molecular mechanisms involved in testis development, spermatogenesis and the processes relating to human foetal testis growth, they have significant limitations as model for human TGCT research. The absence of a mouse model developing GCNIS and a seminoma-type tumours (62) restricts investigations of TGCT formation and acquisition of metastatic potential to primary tissue materials and human cell lines. The identification of SNAI1 and SNAI2 in TGCTs through histological analyses of human samples have prompted us to examine whether they may contribute to tumour cell behaviours.

Author Manuscript

This article is protected by copyright. All rights reserved

By tightly controlling gene transcription, Snail factors promote changes in cell physiology to facilitate the gain of malignant properties in several cells, including breast, gastric, colon and prostate (63). Using the TCam-2 tumour cell line as an *in vitro* model, our functional studies identified distinct roles for SNAI1 in facilitating migration and SNAI2 in supporting viability of seminoma cells. SNAI1 was necessary for maximal TCam-2 cell migration in a wound healing assay, in accordance with studies performed with prostate tumour models (64, 65). SNAI2 downregulation increased TCam-2 cell death, consequently affecting their capacity to adhere and migrate. The role of SNAI2 as a pro-survival factor was previously delineated during development of neural crest cells (66), in gastrointestinal stromal tumour cells (67), and in prostate cancer cell lines (68); in these cells, SNAI2 antagonised apoptosis through the regulation of caspases or repression of pro-apoptotic markers, such as PUMA (69). Although it was shown during mouse chondrogenesis that SNAI1 and SNAI2 functionally compensate for each other's loss (52), their reciprocal regulation was not observed in seminoma cells. We reported that by reducing *SNAI1*, *SNAI2* increased in TCam-2 cells, not *vice-versa*. This resulted in survival of TCam-2 cells lacking *SNAI1*, although increased *SNAI2* levels did not rescue cell migration. These outcomes reinforce the understanding that SNAI1 and SNAI2 are functionally different (70) despite having highly similar protein structures (1).

Each Snail factor is regulated by different signalling pathways, including those mediated by the TGF-β superfamily ligands (reviewed in (10)). These ligands are broadly required during normal embryonic development and late stages of tumorigenesis, where TGF-β activation upregulates Snail factors to promote EMT (71). Phosphorylated SMADs and transcripts encoding ACVR1A, ACVR1B, BMPR1A and BMPR2 are detectable within seminomas (38), indicating that TGF-β signalling is active. Primary cultures of seminoma testis fragments responded to activin A, resulting in a decrease in *KIT* mRNA and protein (72). TCam-2 cell exposure to activin A or to BMP4 promoted proliferation or survival, respectively (41), suggesting that TGF-β superfamily signalling activity can influence seminoma progression. Here we showed that *SNAI2*, but not *SNAI1*, dramatically increased in TCam-2 cells following exposure to BMP4 for 48 hrs (Fig. 4), revealing *SNAI2* as a BMP4 downstream target. To reinforce this, we selectively manipulated the BMP4 signalling pathway by knockdown of IPO5, and thereby drastically reduced the capacity for BMP4 exposure to elevate *SNAI2*. These new findings extend our previous report that showed BMP4 supports TCam-2 cell survival (41) by revealing *SNAI2* as a BMP4 downstream target that mediates BMP4-induced survival in seminoma cells. The variable distribution of IPO5 between the cytoplasm and nucleus, present

This article is protected by copyright. All rights reserved

Author Manuscript

in individual seminoma cells suggests this may indicate different levels of BMP4 signalling; cytoplasmic IPO5 would be expected to perform the canonical nucleocytoplasmic transport role of shuttling transcription factors into the nucleus (73-75), whereas nuclear IPO5 has been shown to indirectly modulate gene transcription (76). Despite a previous report that activin A increases *SNAI2* during placental development (43), it did not regulate Snail levels in TCam-2 cells. More remains to be learned about the fine-tuning of TGF-β signalling in TGCTs, including how they interact to effect transcription of different downstream targets.

The novel observations from this study provide evidence that SNAI1 and SNAI2 are important for both normal and neoplastic germ cell functions. Their concurrent expression in seminoma cells indicate that SNAI1 and SNAI2 may support the induction and maintenance of the tumour phenotype. In conclusion, we propose that minimising SNAI2, but not SNAI1, levels repress BMP4-induced survival of seminoma cells, suggesting that SNAI2 is a potential therapeutic target.

Acknowledgments: The authors would like to thank Dr. Maciej Szarek for technical support, Sarah Moody for provision of materials, and Dr. Liza O'Donnell for expert advice on germ cell identification in the normal adult human testis.

Author Contributions:

Diana J, Micati: Study conception and design, experimental data acquisition, analysis and interpretation, manuscript writing, manuscript revision, final manuscript approval.

Karthika Radhakrishnan: experimental data acquisition, manuscript revision and final manuscript approval.

Julia C. Young: Study design, data analysis and interpretation, manuscript revision and final manuscript approval.

Ewa Rajpert-De Meyts: provision of key materials, manuscript revision and final manuscript approval.

Gary R. Hime: Study conception and design, experimental analysis and data interpretation, manuscript revision, final manuscript approval.

Helen E. Abud: Study conception and design, experimental analysis and data interpretation, manuscript revision, final manuscript approval.

This article is protected by copyright. All rights reserved

Author Manuscript

Kate L. Loveland: Study conception and design, experimental analysis and data interpretation, manuscript writing and revision, final manuscript approval.

Compliance with ethical standards: All procedures involving normal adult human testis and TGCT samples were approved by the Monash University Human Research Ethics Committee and the Regional Committee for Medical Research Ethics (Copenhagen), respectively.

Conflict of interest: The authors have no conflicts of interest in presenting information and material described in this paper.

References

1. Nieto MA. The snail superfamily of zinc-finger transcription factors. Nature reviews Molecular cell biology. 2002;3(3):155-66.
2. Lin Y, Dong C, Zhou BP. Epigenetic regulation of EMT: the Snail story. Current pharmaceutical design. 2014;20(11):1698-705.
3. Kataoka H, Murayama T, Yokode M, Mori S, Sano H, Ozaki H, et al. A novel snail-related transcription factor Smuc regulates basic helix-loop-helix transcription factor activities via specific E-box motifs. Nucleic acids research. 2000;28(2):626-33.
4. Chiang C, Ayyanathan K. Snail/Gfi-1 (SNAG) family zinc finger proteins in transcription regulation, chromatin dynamics, cell signaling, development, and disease. Cytokine & growth factor reviews. 2013;24(2):123-31.
5. Kanarek N, Horwitz E, Mayan I, Leshets M, Cojocaru G, Davis M, et al. Spermatogenesis rescue in a mouse deficient for the ubiquitin ligase SCF{beta}-TrCP by single substrate depletion. Genes & development. 2010;24(5):470-7.
6. Perez-Losada J, Sanchez-Martin M, Rodriguez-Garcia A, Sanchez ML, Orfao A, Flores T, et al. Zinc-finger transcription factor Slug contributes to the function of the stem cell factor c-kit signaling pathway. Blood. 2002;100(4):1274-86.
7. Micati DJ, Hime GR, McLaughlin EA, Abud HE, Loveland KL. Differential expression profiles of conserved Snail transcription factors in the mouse testis. Andrology. 2018;6(2):362-73.
8. Mu W, Starmer J, Fedoriw AM, Yee D, Magnuson T. Repression of the soma-specific transcriptome by Polycomb-repressive complex 2 promotes male germ cell development. Genes & development. 2014;28(18):2056-69.
9. Myrick DA, Christopher MA, Scott AM, Simon AK, Donlin-Asp PG, Kelly WG, et al. KDM1A/LSD1 regulates the differentiation and maintenance of spermatogonia in mice. PloS one. 2017;12(5):e0177473.
10. Wu Y, Zhou BP. Snail: More than EMT. Cell Adh Migr. 2010;4(2):199-203.

This article is protected by copyright. All rights reserved

Author Manuscript

11. Wang Y, Shi J, Chai K, Ying X, Zhou BP. The Role of Snail in EMT and Tumorigenesis. Current cancer drug targets. 2013;13(9):963-72.
12. Batlle E, Sancho E, Franci C, Dominguez D, Monfar M, Baulida J, et al. The transcription factor snail is a repressor of E-cadherin gene expression in epithelial tumour cells. Nature cell biology. 2000;2(2):84-9.
13. Horvay K, Jarde T, Casagranda F, Perreau VM, Haigh K, Nefzger CM, et al. Snai1 regulates cell lineage allocation and stem cell maintenance in the mouse intestinal epithelium. The EMBO journal. 2015;34(10):1319-35.
14. Horvay K, Casagranda F, Gany A, Hime GR, Abud HE. Wnt signaling regulates Snai1 expression and cellular localization in the mouse intestinal epithelial stem cell niche. Stem Cells Dev. 2011;20(4):737-45.
15. Chen YC, Chen YW, Hsu HS, Tseng LM, Huang PI, Lu KH, et al. Aldehyde dehydrogenase 1 is a putative marker for cancer stem cells in head and neck squamous cancer. Biochem Biophys Res Commun. 2009;385(3):307-13.
16. Zhou W, Lv R, Qi W, Wu D, Xu Y, Liu W, et al. Snail contributes to the maintenance of stem cell-like phenotype cells in human pancreatic cancer. PloS one. 2014;9(1):e87409.
17. Jones RJ, Matsui WH, Smith BD. Cancer stem cells: are we missing the target? J Natl Cancer Inst. 2004;96(8):583-5.
18. Yang HW, Menon LG, Black PM, Carroll RS, Johnson MD. SNAI2/Slug promotes growth and invasion in human gliomas. BMC Cancer. 2010;10:301.
19. Kim S, Yao J, Suyama K, Qian X, Qian BZ, Bandyopadhyay S, et al. Slug promotes survival during metastasis through suppression of Puma-mediated apoptosis. Cancer research. 2014;74(14):3695-706.
20. Skakkebaek NE. Abnormal morphology of germ cells in two infertile men. Acta Pathol Microbiol Scand A. 1972;80(3):374-8.
21. Rajpert-De Meyts E. Developmental model for the pathogenesis of testicular carcinoma in situ: genetic and environmental aspects. Hum Reprod Update. 2006;12(3):303-23.
22. Looijenga LH, Gillis AJ, Stoop H, Biermann K, Oosterhuis JW. Dissecting the molecular pathways of (testicular) germ cell tumour pathogenesis; from initiation to treatment-resistance. International journal of andrology. 2011;34(4 Pt 2):e234-51.
23. Ulbright TM. Germ cell neoplasms of the testis. Am J Surg Pathol. 1993;17(11):1075-91.
24. Ferlay J, Soerjomataram I, Dikshit R, Eser S, Mathers C, Rebelo M, et al. Cancer incidence and mortality worldwide: sources, methods and major patterns in GLOBOCAN 2012. Int J Cancer. 2015;136(5):E359-86.

This article is protected by copyright. All rights reserved

Author Manuscript

25. Williamson SR, Delahunt B, Magi-Galluzzi C, Algaba F, Egevad L, Ulbright TM, et al. The World Health Organization 2016 classification of testicular germ cell tumours: a review and update from the International Society of Urological Pathology Testis Consultation Panel. Histopathology. 2017;70(3):335-46.
26. Itman C, Wong C, Whiley PA, Fernando D, Loveland KL. TGFbeta superfamily signaling regulators are differentially expressed in the developing and adult mouse testis. Spermatogenesis. 2011;1(1):63-72.
27. Le Bras GF, Loomans HA, Taylor CJ, Revetta FL, Andl CD. Activin A balance regulates epithelial invasiveness and tumorigenesis. Lab Invest. 2014;94(10):1134-46.
28. Alarmo EL, Huhtala H, Korhonen T, Pylkkanen L, Holli K, Kuukasjarvi T, et al. Bone morphogenetic protein 4 expression in multiple normal and tumor tissues reveals its importance beyond development. Mod Pathol. 2013;26(1):10-21.
29. Wang RN, Green J, Wang Z, Deng Y, Qiao M, Peabody M, et al. Bone Morphogenetic Protein (BMP) signaling in development and human diseases. Genes Dis. 2014;1(1):87-105.
30. Hill CS. Transcriptional Control by the SMADs. Cold Spring Harb Perspect Biol. 2016;8(10).
31. Tsuchida K, Nakatani M, Hitachi K, Uezumi A, Sunada Y, Ageta H, et al. Activin signaling as an emerging target for therapeutic interventions. Cell Commun Signal. 2009;7:15.
32. Loveland KL, Major AT, Butler R, Young JC, Jans DA, Miyamoto Y. Putting things in place for fertilization: discovering roles for importin proteins in cell fate and spermatogenesis. Asian J Androl. 2015;17(4):537-44.
33. Hogarth C, Itman C, Jans DA, Loveland KL. Regulated nucleocytoplasmic transport in spermatogenesis: a driver of cellular differentiation? Bioessays. 2005;27(10):1011-25.
34. Hogarth CA, Jans DA, Loveland KL. Subcellular distribution of importins correlates with germ cell maturation. Dev Dyn. 2007;236(8):2311-20.
35. Whiley PA, Miyamoto Y, McLachlan RI, Jans DA, Loveland KL. Changing subcellular localization of nuclear transport factors during human spermatogenesis. International journal of andrology. 2012;35(2):158-69.
36. Baas R, Sijm A, van Teeffelen HA, van Es R, Vos HR, Marc Timmers HT. Quantitative Proteomics of the SMAD (Suppressor of Mothers against Decapentaplegic) Transcription Factor Family Identifies Importin 5 as a Bone Morphogenic Protein Receptor SMAD-specific Importin. The Journal of biological chemistry. 2016;291(46):24121-32.
37. Dias V, Meachem S, Rajpert-De Meyts E, McLachlan R, Manuelpillai U, Loveland KL. Activin receptor subunits in normal and dysfunctional adult human testis. Hum Reprod. 2008;23(2):412-20.

Author Manuscript

This article is protected by copyright. All rights reserved

667 38. Dias VL, Rajpert-De Meyts E, McLachlan R, Loveland KL. Analysis of activin/TGFB-signaling
668 modulators within the normal and dysfunctional adult human testis reveals evidence of altered
669 signaling capacity in a subset of seminomas. Reproduction. 2009;138(5):801-11.
670 39. Fustino N, Rakheja D, Ateek CS, Neumann JC, Amatruda JF. Bone morphogenetic protein
671 signalling activity distinguishes histological subsets of paediatric germ cell tumours. International
672 journal of andrology. 2011;34(4 Pt 2):e218-33.
673 40. Neumann JC, Chandler GL, Damoulis VA, Fustino NJ, Lillard K, Looijenga L, et al. Mutation in
674 the type IB bone morphogenetic protein receptor Alk6b impairs germ-cell differentiation and causes
675 germ-cell tumors in zebrafish. Proceedings of the National Academy of Sciences of the United States
676 of America. 2011;108(32):13153-8.
677 41. Young JC, Jaiprakash A, Mithraprabhu S, Itman C, Kitazawa R, Looijenga LH, et al. TCam-2
678 seminoma cell line exhibits characteristic foetal germ cell responses to TGF-beta ligands and retinoic
679 acid. International journal of andrology. 2011;34(4 Pt 2):e204-17.
680 42. Sonne SB, Almstrup K, Dalgaard M, Juncker AS, Edsgard D, Ruban L, et al. Analysis of gene
681 expression profiles of microdissected cell populations indicates that testicular carcinoma in situ is an
682 arrested gonocyte. Cancer research. 2009;69(12):5241-50.
683 43. Li Y, Klausen C, Zhu H, Leung PC. Activin A Increases Human Trophoblast Invasion by Inducing
684 SNAIL-Mediated MMP2 Up-Regulation Through ALK4. J Clin Endocrinol Metab. 2015;100(11):E1415-
685 27.
686 44. Kestens C, Siersema PD, Offerhaus GJ, van Baal JW. Correction: BMP4 Signaling Is Able to
687 Induce an Epithelial-Mesenchymal Transition-Like Phenotype in Barrett's Esophagus and Esophageal
688 Adenocarcinoma through Induction of SNAIL2. PloS one. 2016;11(6):e0158755.
689 45. Mizuno Y, Gotoh A, Kamidono S, Kitazawa S. [Establishment and characterization of a new
690 human testicular germ cell tumor cell line (TCam-2)]. Nihon Hinyokika Gakkai Zasshi.
691 1993;84(7):1211-8.
692 46. de Jong J, Stoop H, Gillis AJ, Hersmus R, van Gurp RJ, van de Geijn GJ, et al. Further
693 characterization of the first seminoma cell line TCam-2. Genes Chromosomes Cancer.
694 2008;47(3):185-96.
695 47. Chang KK, Yoon C, Yi BC, Tap WD, Simon MC, Yoon SS. Platelet-derived growth factor
696 receptor-alpha and -beta promote cancer stem cell phenotypes in sarcomas. Oncogenesis.
697 2018;7(6):47.
698 48. De Craene B, Denecker G, Vermassen P, Taminau J, Mauch C, Derore A, et al. Epidermal Snail
699 expression drives skin cancer initiation and progression through enhanced cytoprotection, epidermal

Author Manuscript

This article is protected by copyright. All rights reserved

stem/progenitor cell expansion and enhanced metastatic potential. Cell Death Differ. 2014;21(2):310-20.
49. Lu ZY, Dong R, Li D, Li WB, Xu FQ, Geng Y, et al. SNAI1 overexpression induces stemness and promotes ovarian cancer cell invasion and metastasis. Oncology reports. 2012;27(5):1587-91.
50. Hwang WL, Yang MH, Tsai ML, Lan HY, Su SH, Chang SC, et al. SNAIL regulates interleukin-8 expression, stem cell-like activity, and tumorigenicity of human colorectal carcinoma cells. Gastroenterology. 2011;141(1):279-91, 91 e1-5.
51. Kim S, Gunesdogan U, Zylicz JJ, Hackett JA, Cougot D, Bao S, et al. PRMT5 protects genomic integrity during global DNA demethylation in primordial germ cells and preimplantation embryos. Molecular cell. 2014;56(4):564-79.
52. Chen Y, Gridley T. Compensatory regulation of the Snai1 and Snai2 genes during chondrogenesis. Journal of bone and mineral research : the official journal of the American Society for Bone and Mineral Research. 2013;28(6):1412-21.
53. Voog J, Sandall SL, Hime GR, Resende LP, Loza-Coll M, Aslanian A, et al. Escargot restricts niche cell to stem cell conversion in the Drosophila testis. Cell Rep. 2014;7(3):722-34.
54. Hammoud SS, Low DH, Yi C, Carrell DT, Guccione E, Cairns BR. Chromatin and transcription transitions of mammalian adult germline stem cells and spermatogenesis. Cell stem cell. 2014;15(2):239-53.
55. Hammoud SS, Low DH, Yi C, Lee CL, Oatley JM, Payne CJ, et al. Transcription and imprinting dynamics in developing postnatal male germline stem cells. Genes & development. 2015;29(21):2312-24.
56. Kanatsu-Shinohara M, Shinohara T. Spermatogonial stem cell self-renewal and development. Annu Rev Cell Dev Biol. 2013;29:163-87.
57. La HM, Makela JA, Chan AL, Rossello FJ, Nefzger CM, Legrand JMD, et al. Identification of dynamic undifferentiated cell states within the male germline. Nat Commun. 2018;9(1):2819.
58. von Kopylow K, Schulze W, Salzbrunn A, Spiess AN. Isolation and gene expression analysis of single potential human spermatogonial stem cells. Molecular human reproduction. 2016;22(4):229-39.
59. Guo J, Grow EJ, Yi C, Mlcochova H, Maher GJ, Lindskog C, et al. Chromatin and Single-Cell RNA-Seq Profiling Reveal Dynamic Signaling and Metabolic Transitions during Human Spermatogonial Stem Cell Development. Cell stem cell. 2017;21(4):533-46 e6.
60. Hermann BP, Cheng K, Singh A, Roa-De La Cruz L, Mutoji KN, Chen IC, et al. The Mammalian Spermatogenesis Single-Cell Transcriptome, from Spermatogonial Stem Cells to Spermatids. Cell Rep. 2018;25(6):1650-67 e8.

This article is protected by copyright. All rights reserved

Author Manuscript

61. Tan K, Wilkinson MF. Human Spermatogonial Stem Cells Scrutinized under the Single-Cell Magnifying Glass. Cell stem cell. 2019;24(2):201-3.
62. Zechel JL, MacLennan GT, Heaney JD, Nadeau JH. Spontaneous metastasis in mouse models of testicular germ-cell tumours. International journal of andrology. 2011;34(4 Pt 2):e278-87.
63. Kaufhold S, Bonavida B. Central role of Snail1 in the regulation of EMT and resistance in cancer: a target for therapeutic intervention. Journal of experimental & clinical cancer research : CR. 2014;33:62.
64. Li H, Li M, Xu D, Zhao C, Liu G, Wang F. Overexpression of Snail in retinal pigment epithelial triggered epithelial-mesenchymal transition. Biochem Biophys Res Commun. 2014;446(1):347-51.
65. Osorio LA, Farfan NM, Castellon EA, Contreras HR. SNAIL transcription factor increases the motility and invasive capacity of prostate cancer cells. Mol Med Rep. 2016;13(1):778-86.
66. Tribulo C, Aybar MJ, Sanchez SS, Mayor R. A balance between the anti-apoptotic activity of Slug and the apoptotic activity of msx1 is required for the proper development of the neural crest. Developmental biology. 2004;275(2):325-42.
67. Pulkka OP, Nilsson B, Sarlomo-Rikala M, Reichardt P, Eriksson M, Hall KS, et al. SLUG transcription factor: a pro-survival and prognostic factor in gastrointestinal stromal tumour. British journal of cancer. 2017;116(9):1195-202.
68. Emadi Baygi M, Soheili ZS, Essmann F, Deezagi A, Engers R, Goering W, et al. Slug/SNAI2 regulates cell proliferation and invasiveness of metastatic prostate cancer cell lines. Tumour Biol. 2010;31(4):297-307.
69. Wu WS, Heinrichs S, Xu D, Garrison SP, Zambetti GP, Adams JM, et al. Slug antagonizes p53-mediated apoptosis of hematopoietic progenitors by repressing puma. Cell. 2005;123(4):641-53.
70. Villarejo A, Cortes-Cabrera A, Molina-Ortiz P, Portillo F, Cano A. Differential role of Snail1 and Snail2 zinc fingers in E-cadherin repression and epithelial to mesenchymal transition. The Journal of biological chemistry. 2014;289(2):930-41.
71. Saitoh M, Miyazawa K. Transcriptional and post-transcriptional regulation in TGF-beta-mediated epithelial-mesenchymal transition. J Biochem. 2012;151(6):563-71.
72. Jorgensen A, Young J, Nielsen JE, Joensen UN, Toft BG, Rajpert-De Meyts E, et al. Hanging drop cultures of human testis and testis cancer samples: a model used to investigate activin treatment effects in a preserved niche. British journal of cancer. 2014;110(10):2604-14.
73. Nakatani T, Yamagata K, Kimura T, Oda M, Nakashima H, Hori M, et al. Stella preserves maternal chromosome integrity by inhibiting 5hmC-induced gammaH2AX accumulation. EMBO Rep. 2015;16(5):582-9.

Author Manuscript

This article is protected by copyright. All rights reserved

74. Heese K, Yamada T, Akatsu H, Yamamoto T, Kosaka K, Nagai Y, et al. Characterizing the new transcription regulator protein p60TRP. J Cell Biochem. 2004;91(5):1030-42.
75. Swale C, Monod A, Tengo L, Labaronne A, Garzoni F, Bourhis JM, et al. Structural characterization of recombinant IAV polymerase reveals a stable complex between viral PA-PB1 heterodimer and host RanBP5. Sci Rep. 2016;6:24727.
76. Clerman A, Noor Z, Fishelevich R, Lockatell V, Hampton BS, Shah NG, et al. The full-length interleukin-33 (FLIL33)-importin-5 interaction does not regulate nuclear localization of FLIL33 but controls its intracellular degradation. The Journal of biological chemistry. 2017;292(52):21653-61.

Figures

Figure SNAI1 and SNAI2 are present in normal and neoplastic human testis samples.

In situ hybridisation with *SNAI1* antisense cRNA probe detected *SNAI1* transcript in normal adult human testis (A), GCNIS (D), and seminoma (F) samples. Immunocytochemical staining revealed *SNAI2* mRNA (B) and protein (C) in the normal adult human testis, and SNAI2 protein in GCNIS (E) and seminoma (G) samples. Primary antibody was omitted in negative control (insert). Blue arrow = spermatogonia; green arrow = spermatocytes; white arrow = spermatids; grey arrow = Sertoli cells; red arrow = peritubular cells; yellow arrow = interstitial cells; purple arrow = GCNIS cells; orange arrow = seminoma cells; pink arrow = immune cell infiltrates. Scale bar = 10 μm.

Figure 2 SNAI1 and SNAI2 in TCam-2 cells, and evidence of reciprocal expression. (A) Immunofluorescence identified SNAI1 and SNAI2 in TCam-2 cell nuclei. Scale bar = 10 μm. (B, C) siRNA knockdown of *SNAI1* (B) and *SNAI2* (C). Knockdown efficiency and *SNAI1/SNAI2* reciprocal regulation were each documented at 1 (t 1) and 4 (t 4) days post-transfections. The SCRAM siRNA construct served as transfection control. Graphs are presented as mean values, with error bars representing SEM, and significance was determined using the Mann-Whitney test. *$p < 0.05$, $n = 3$.

Figure 3 SNAI1 and SNAI2 differentially affect TCam-2 cell behaviour. TCam-2 cells were transfected with *SNAI1*, *SNAI2* and *SCRAM* siRNA constructs to measure: (A) migration, (B) viability, (C) adhesion, and proliferation by BrdU incorporation (D) and xCElligence real-time

This article is protected by copyright. All rights reserved

Author Manuscript

analysis (E). Graphs present mean values, with error bars representing the SEM. For viability, adhesion and proliferation assays, significance was determined using the Mann-Whitney test, * $p < 0.05$. For migration, non-parametric ANOVA and Tukey's multiple comparison test determined significance, * $p < 0.05$.

Figure 4 BMP4-induced survival and migration of TCam-2 cells is reduced by SNAI2 inhibition. (A, B) Changes in *SNAI1* and *SNAI2* transcript levels following activin A (AA) and BMP4 treatments were assessed by qRT-PCR. (C, D) Immunohistochemical analysis revealed that IPO5 subcellular localisation was heterogenous in seminomas (n = 4). Primary antibody was omitted in negative controls (inserts; c, d). Scale bar = 10 μm. (E, F) TCam-2 cells transfected with *IPO5* siRNA construct were treated with vehicle control, AA or BMP4, then *SNAI1* and *SNAI2* levels were measured by qRT-PCR. *Sc* siRNA and vehicle were used as transfection and treatment controls, respectively. Each value was normalised to *RPLP0*. Graphs present mean values; error bars indicate SEM. Statistical analysis was performed relative to the vehicle control. Significance was calculated using the Mann-Whitney test, * $p < 0.05$. (G - I) TCam-2 cells transfected with *SNAI2* (G-I) or *IPO5* (J, K) siRNA constructs were treated with vehicle control, AA or BMP4, then effects on migration were measured. Wound area is presented relative to the gap measured at time point 0. *Sc* siRNA and vehicle were used as transfection and treatment controls, respectively. Graphs are presented as mean values, with error bars indicating SEM, and significance was determined through 2-way Anova. * $p < 0.05$, n = 3.

Fig. S1. Expression of *SNAI1* transcript in the normal adult and neoplastic human testis. Purple staining indicates the cellular sites of *SNAI1* mRNA synthesis in the additional normal adult (A) and neoplastic human testis (B – E) samples. Within the second normal adult human testis sample Blue arrow = spermatogonia; green arrow = spermatocytes; grey arrow = Sertoli cells; red arrow = peritubular cells; yellow arrow = interstitial cells; purple arrow = GCNIS cells; orange arrow = seminoma cells; pink arrow = immune cell infiltrates. Scale bar = 10 μm.

Fig. S2. SNAI2 localisation in the normal adult and neoplastic human testis. Brown staining indicates SNAI2 protein localisation in the normal adult human testis (A), GCNIS (B, C), and seminoma (D, E) samples. Intense background signal is evident within the interstitium of the normal adult human and GCNIS testis samples. Blue arrow = spermatogonia; green

This article is protected by copyright. All rights reserved

Author Manuscript

arrow = spermatocytes; white arrow = spermatids; grey arrow = Sertoli cells; red arrow = peritubular cells; yellow arrow = interstitial cells; purple arrow = GCNIS cells; orange arrow = seminoma cells; pink arrow = immune cell infiltrates. Scale bar = 10 μm.

Fig. S3. **Dose-response of activin A and BMP4 on Snail transcript levels**. Serum-starved TCam-2 cells were treated with increasing dose of activin A and BMP4. Forty-eight hours post-treatment, *SNAI1* (A, B) and *SNAI2* (C, D) transcript levels were measured. Graphs show the mean values. These experiments were repeated twice.

Fig. S4 IPO5 protein localisation in TGCT samples, and *IPO5* and *Snail* expression in TCam-2 cells. (A - E) IPO5 subcellular localisation in GCNIS (A – C) and seminoma (D, E) samples was heterogeneous. **(F) *SNAI1*, *SNAI2*, *SNAI3* and *IPO5* were measured in two TCam-2 cell samples**. The Surani RNASeq demonstrated that *SNAI1, SNAI2* and *IPO5,* not *SNAI3,* are detectable in TCam-2 cells. **(G) *IPO5* knockdown in TCam-2 cells**. TCam-2 cells were transfected for 24 hrs with 12.5 pmol of *SCRAM* control and *IPO5* siRNA constructs, then treated with 5 ng/ml of vehicle control, AA or BMP4. Knockdown efficiency was measured 48 hrs post-treatment. Graphs show mean values, with error bars representing SEM. Significance was determined using the Mann-Whitney test. *$p < 0.05$, $n = 3$. Purple arrow = GCNIS cells; grey arrow = Sertoli cells; orange arrow = seminoma cells. Scale bars = 10 μm.

Author Manuscript

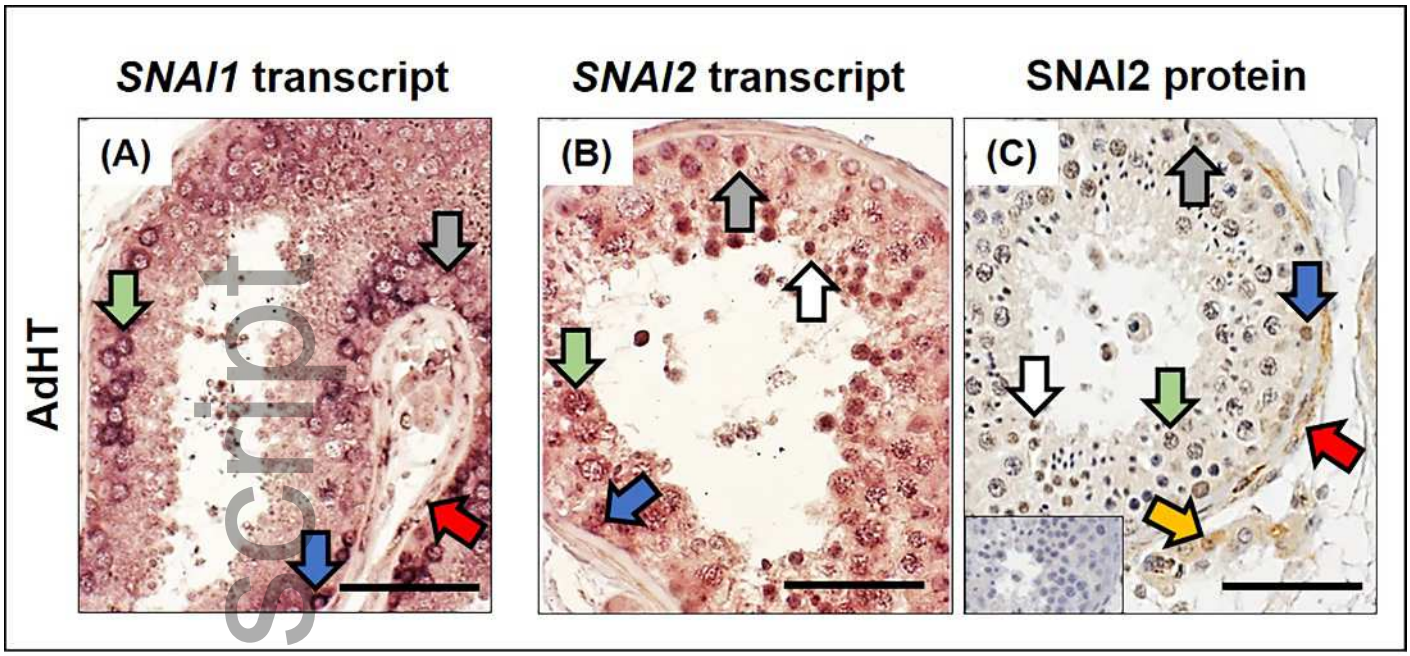
This article is protected by copyright. All rights reserved

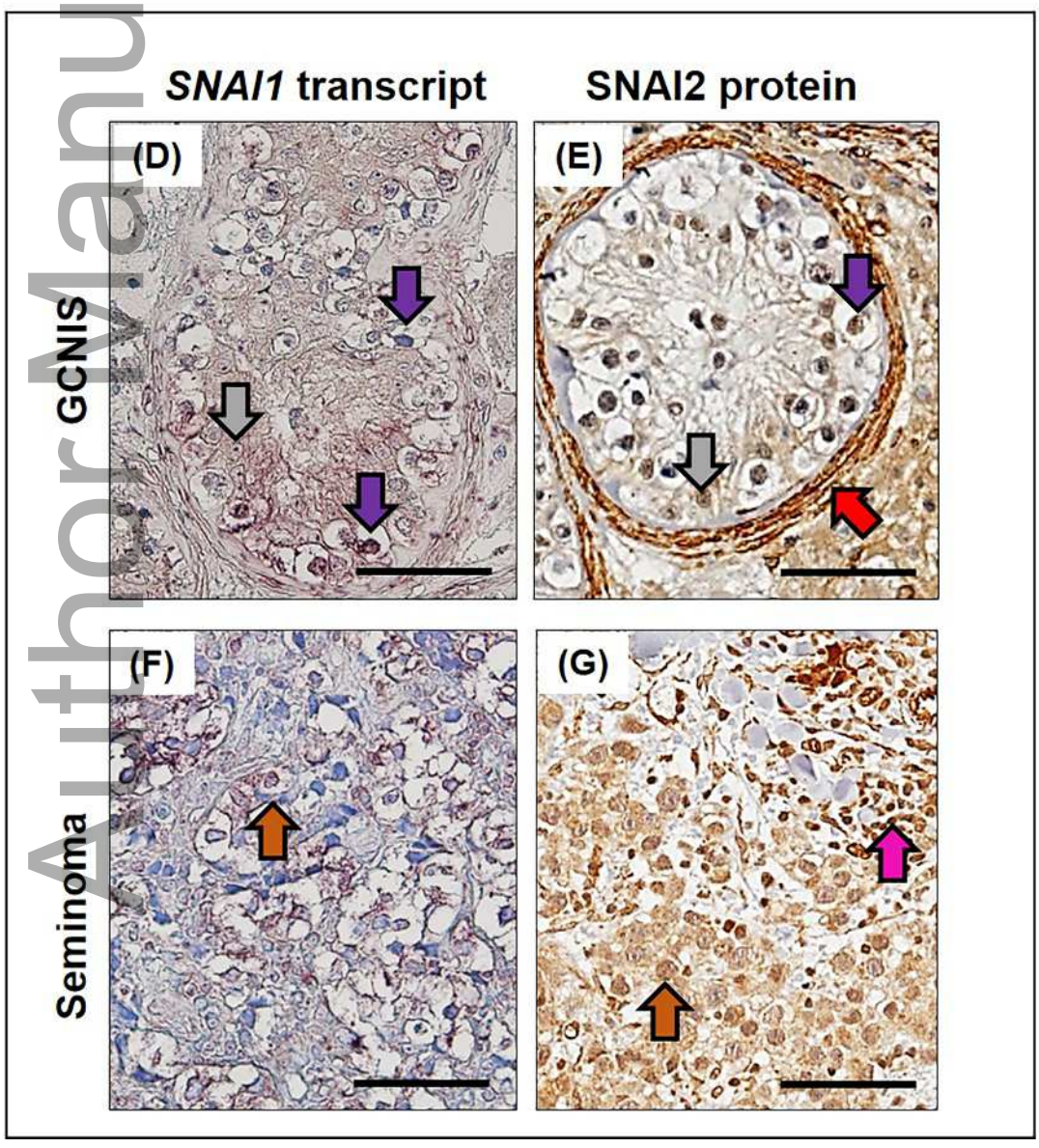
Gene	Accession number	Forward (5'-3')	Reverse (5'-3')	Technique
SNAI1	NM_005985	CTGCGTGGGTTTTTGTATCC	TCGGGGCATCTCAGACTCTA	*in situ* hybridisation
SNAI2	NM_003068	GAGAGCTGCAAGAGCATGGA	TTGCTGCCAAATCATTTCAA	*in situ* hybridisation
RPLP0	NM_001002	CTATCATCAACGGGTACAAACGAG	CAGATGGATCAGCCAAGAAGG	qRT-PCR
SNAI1	NM_005985	TAGCGAGTGGTTCTTCTGCG	AGGGCTGCTGGAAGGTAAAC	qRT-PCR
SNAI2	NM_003068	ACAGCGAACTGGACACACAT	GCGGTAGTCCACACAGTGAT	qRT-PCR
IPO5	NM_178310	AGGTCCTTCCACACTGGTTG	AATTGCCTCGTGCATTTCTC	qRT-PCR

Table 1. Primer sequences used for generation of in situ hybridisation probes and for qRT-PCR to detect mouse and human transcripts.

Author Manuscript

This article is protected by copyright. All rights reserved

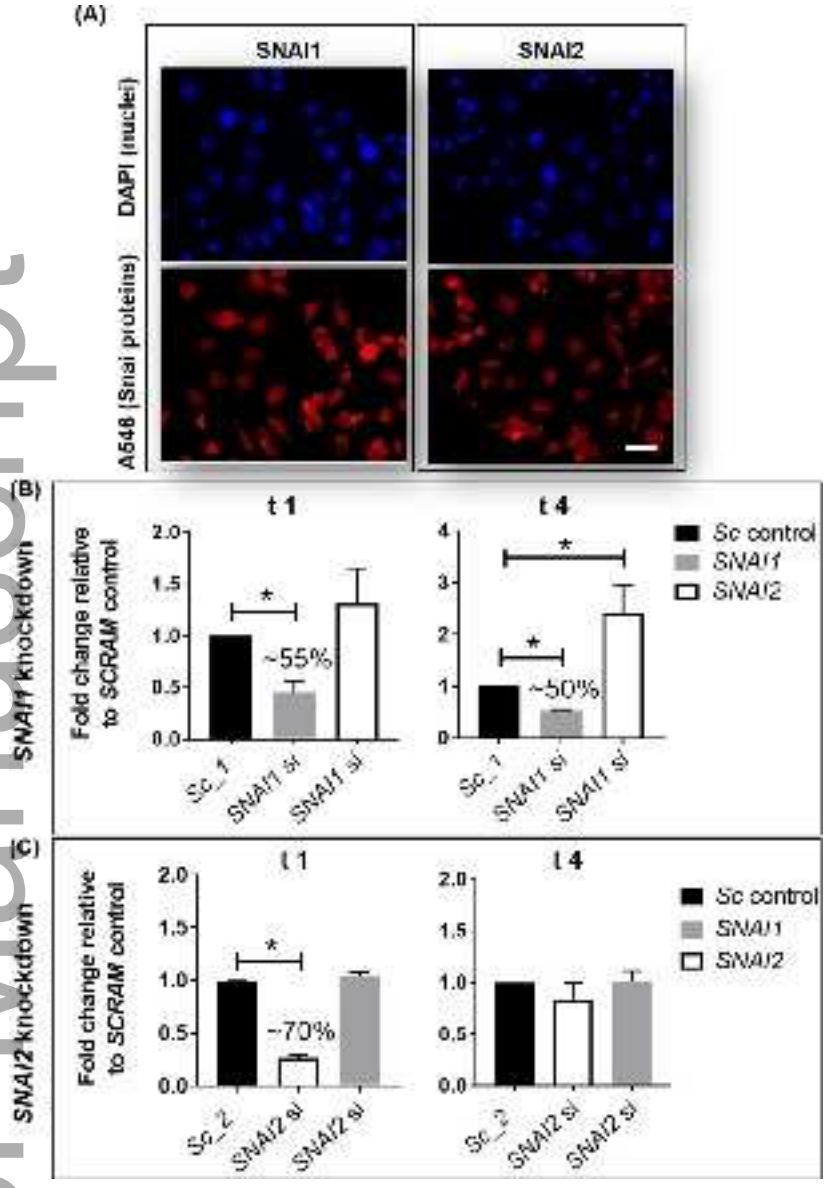




Author Manuscript

This article is protected by copyright. All rights reserved

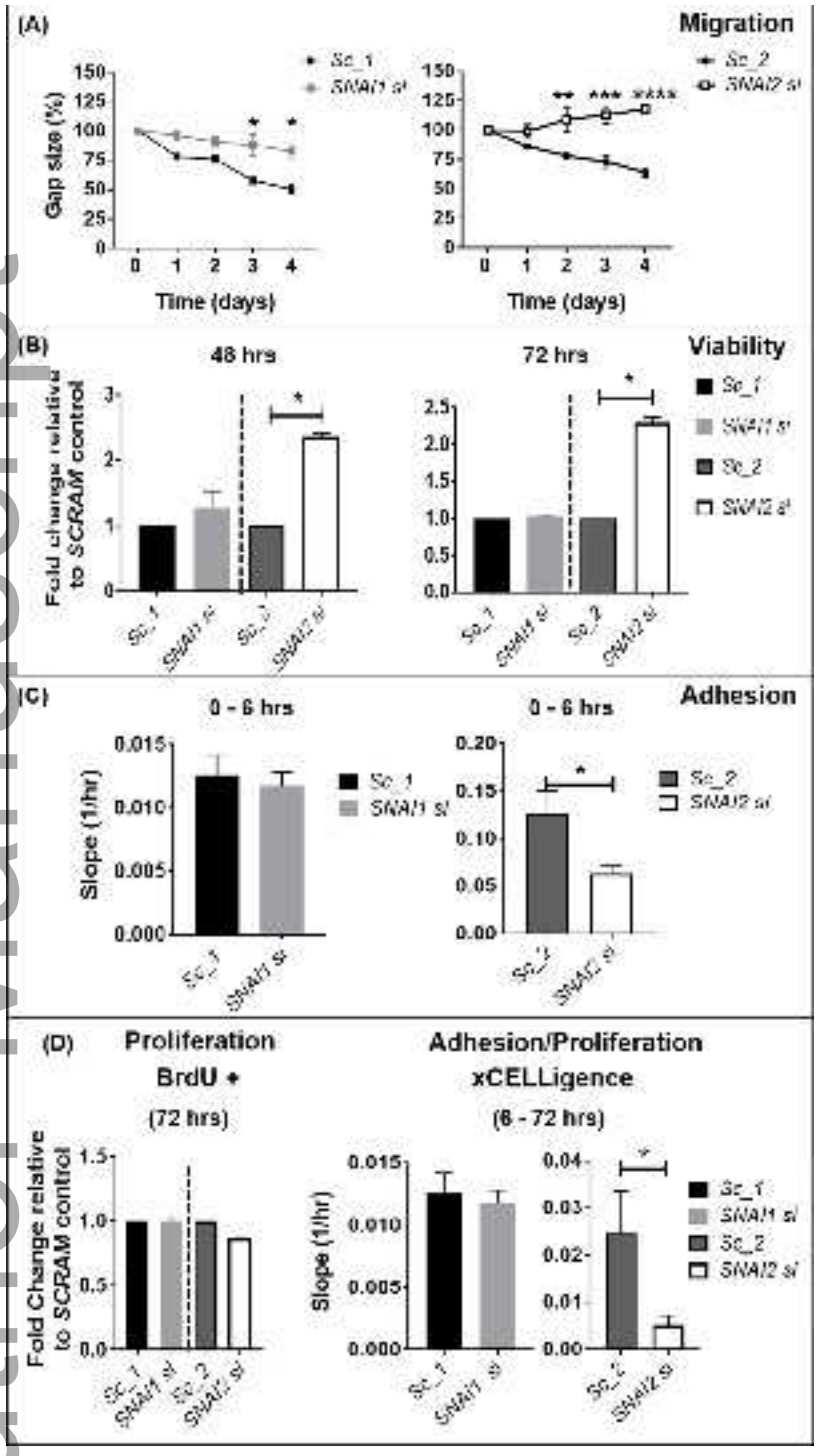
Author Manuscript



andr_12823_f2.tif

This article is protected by copyright. All rights reserved

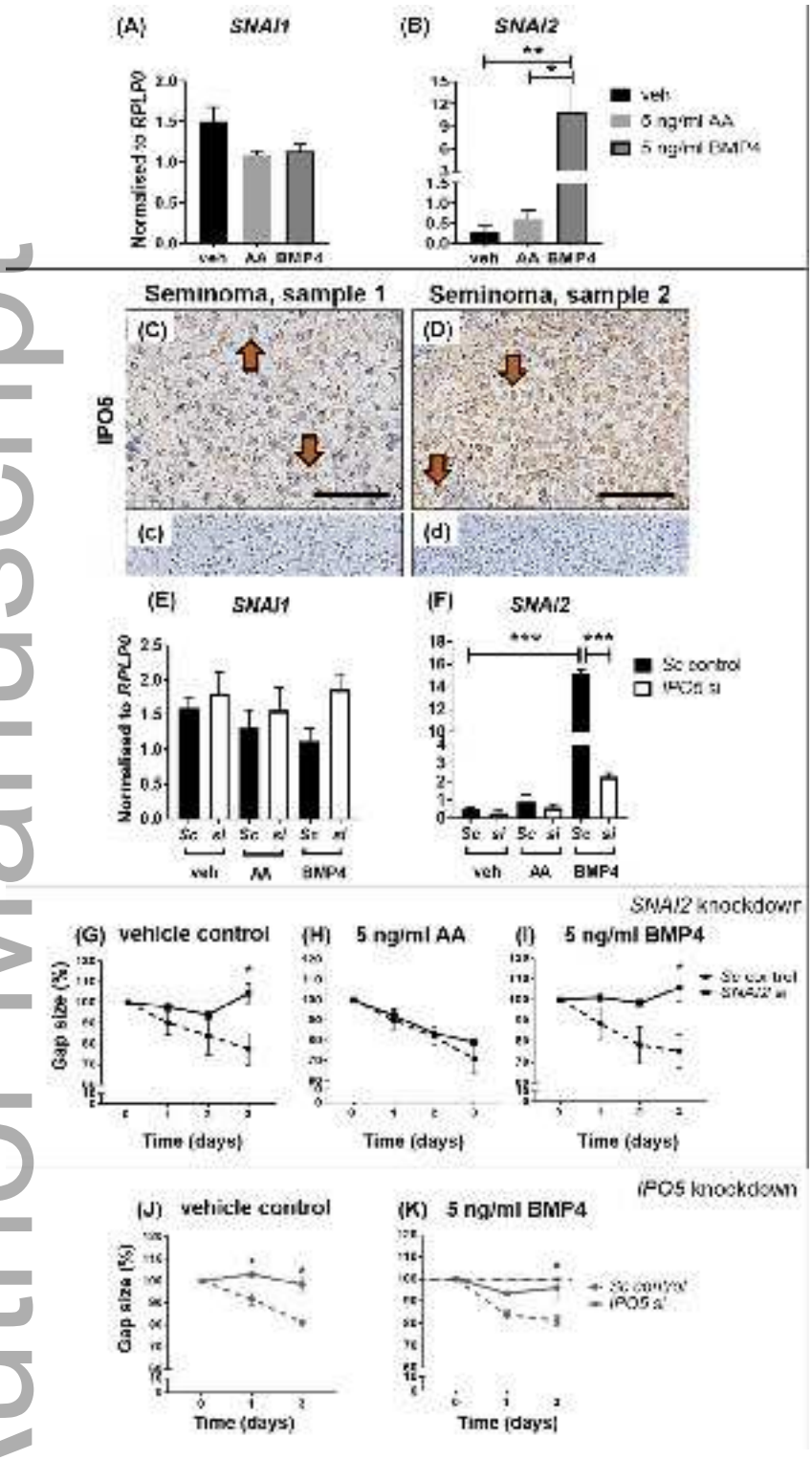
Author Manuscript



andr_12823_f3.tif

This article is protected by copyright. All rights reserved

Author Manuscript



andr_12823_f4.tif

This article is protected by copyright. All rights reserved